

Incorporation of VOC-Selective Peptides in Gas Sensing Materials

Ana Rita Oliveira^{1,2}^a, Efthymia Ramou^{1,2}^b, Gonçalo D. G. Teixeira^{1,2}^c,
Susana I. C. J. Palma^{1,2}^d and Ana C. A. Roque^{1,2*}^e

¹Associate Laboratory i4HB- Institute for Health and Bioeconomy, School of Science and Technology,
NOVA University Lisbon, 2829-516 Caparica, Portugal

²UCIBIO – Applied Molecular Biosciences Unit, Department of Chemistry, School of Science and Technology,
NOVA University Lisbon, 2829-516 Caparica, Portugal

Keywords: Ionogels, Hybrid Gels, Peptides, Gas Sensing, Electronic Nose.

Abstract: Enhancing the selectivity of gas sensing materials towards specific volatile organic compounds (VOCs) is challenging due to the chemical simplicity of VOCs as well as the difficulty in interfacing VOC selective biological elements with electronic components used in the transduction process. We aimed to tune the selectivity of gas sensing materials through the incorporation of VOC-selective peptides into gel-like gas sensing materials. Specifically, a peptide (P1) known to discriminate single carbon deviations among benzene and derivatives, along with two modified versions (P2 and P3), were integrated with gel compositions containing gelatin, ionic liquid and without or with a liquid crystal component (ionogels and hybrid gels respectively). These formulations change their electrical or optical properties upon VOC exposure, and were tested as sensors in an in-house developed e-nose. Their ability to distinct and identify VOCs was evaluated via a supervised machine learning classifier. Enhanced discrimination of benzene and hexane was detected for the P1-based hybrid gel. Additionally, complementarity of the electrical and optical sensors was observed considering that a combination of both their accuracy predictions yielded the best classification results for the tested VOCs. This indicates that a combinatorial array in a dual-mode e-nose could provide optimal performance and enhanced selectivity.

1 INTRODUCTION

Gas sensing is currently emerging as a critically important technology related to a broad range of applications such as medicine (van Hooren et al., 2016), and early diagnosis of disease (Broza et al., 2015; Cruz et al., 2017; Fitzgerald & Fenniri, 2017; Krilaviciute et al., 2015; Susana I.C.J. Palma et al., 2018; Vishinkin & Haick, 2015). Indeed, volatile organic compounds (VOCs) are becoming increasingly recognized as potential biomarkers associated with disease. Artificial olfaction is the automated simulation of the sense of smell through the use of electronic nose devices (e-noses), comprised by an array of chemical sensors with

partial selectivity coupled with signal-processing and pattern recognition tools. The most common and commercially available gas sensing materials include metal oxide semiconductors (Dey, 2018) or conducting polymers (Park et al., 2017). However, their main drawbacks include low long-term sensor stability, high maintenance, cumbersome and complex instrumentation, and most importantly low selectivity. Thus, it is of high interest to develop better and competitive alternatives, by adapting the components of the sensors in order to enhance their selectivity, reliability and portability (Son et al., 2017). In biological olfaction, odorant binding proteins and olfactory receptors are the main tools used to address the difficult problem of selectivity. In artificial olfaction, these find limitations as they are

^a <https://orcid.org/0000-0001-8496-1746>

^b <https://orcid.org/0000-0003-2376-6749>

^c <https://orcid.org/0000-0001-7675-5926>

^d <https://orcid.org/0000-0002-1851-8110>

^e <https://orcid.org/0000-0002-4586-3024>

difficult to produce, as well as to stabilise and interface with electronic systems for signal transduction, long-term storage and repeated use (Barbosa et al., 2018).

Among the alternative options to tune selectivity, peptides are one of the most attractive choices due to their robustness, chemical diversity, compact size, and their adaptability to extreme environments and safely long-term storage (Cui et al., 2012; Sankaran et al., 2012). Furthermore, they can be developed to bind distinct targets through rational design or discovery by panning of phage display libraries (Kuang et al., 2010).

In this work, we investigated the incorporation of a previously reported peptide (peptide P1), and two designed derivatives (peptides P2 and P3) able to discriminate single carbon deviations among benzene and derivatives such as toluene and xylene (Ju et al., 2015), into gel-like sensing materials yielding electrical and optical signals in the presence of VOCs. Two gel formulations were studied: a gelatin matrix gelled in an ionic liquid environment ([BMIM][DCA]) (ionogels yielding an electrical signal by monitoring the changes in ionic conductance of the formulation) and the same matrix with a liquid crystal component (hybrid gels yielding an optical signal due to their birefringence). The modified versions of P1 were obtained through the addition of non-natural amino acids at the C-terminal - norleucine (Nle - P2 peptide) and biphenylalanine (Bip, - P3 peptide) - with the purpose to facilitate their binding in the ionic liquid-liquid crystal interface, due to their structural resemblance with 5CB (Figure 1). These materials offer the possibility to add the peptide selective moiety with unprecedented simple procedures that take advantage of self-assembly and autonomous compartmentalization, avoiding harsh chemical reactions and peptide covalent attachment onto surfaces.

2 MATERIALS AND METHODS

2.1 Materials and Reagents

Gelatin from bovine skin (gel strength \approx 225 g; Bloom, Type B), was purchased from SigmaAldrich. The liquid crystal 4-cyano-4'-pentylbiphenyl (5CB), was acquired from TCI Europe, and the Ionic liquid 1-Butyl-3-methylimidazolium chloride ([BMIM][DCA], >98%) was purchased from IoLiTec. Peptides 1, 2 and 3 were purchased from Genecust (purity >95,9%). Ethanol (purity 99.8%) and Fluorescein isothiocyanate (FITC) Isomer I (99%

purity) were purchased from Sigma-Aldrich, while benzene, hexane, xylene and toluene were supplied by Fisher Scientific, and acetone (purity 99.5%) was purchased from Honeywell.

2.2 Confirmation of Peptide P1 Binding by Multi-Parametric Surface Plasmon Resonance (MP-SPR)

For the MP-SPR studies, an Au-glass slide was modified with 3-mercaptopropionic acid (3-MPA), a linker with a hydroxyl group and a sulfhydryl group, which binds to the Au surface thiols. For the immobilization of the P1 peptide (10 μ M in 20 mM sodium phosphate solution, at pH 7) on the surface EDC/NHS chemistry was used, and Ethanolamine was used as a blocking agent for extremities where P1 was not bound. This method was used to produce the sample placed in the peptide chamber, whereas the control chamber contained an Au-glass slide with all the previously described functionalization, minus the immobilization of the peptide step. The MP-SPR signal variation within time was measured by using two wavelengths, 670 nm and 785 nm (mDeg), being the average of the signal measured at the two wavelengths defined as Δ mDeg.

2.3 Incorporation of the Peptides into Ionogels

For the production of ionogel sensors we used the same protocol as previously described with the addition of peptide solutions (Abid Hussain et al., 2017). The final formulation was pipetted onto interdigitated golden electrodes deposited on untreated glass slides and spread into a thin film using a TQC film applicator (Automatic Film Applicator Standard, TQC) with a 15 μ m thickness. After production, the peptide ionogels were left to dry on a sealed clean petri dish, in a humidity box with environmental control. Control ionogels (without the incorporation of a peptide component) were also prepared, for comparison purposes.

2.4 Incorporation of the Peptides into Hybrid Gels

Peptide hybrid gels were formulated by mixing all components plus the peptide solution following protocols previously described (C. Esteves et al., 2019; A. Hussain et al., 2017). When gelation occurs, the gel compositions were deposited on top of

untreated glass slides and spread into thin films using a TQC film applicator (Automatic Film Applicator Standard, TQC) with a 30 μm thickness. After production, the gels were stored within an environment of controlled humidity. Control hybrid gels (without a peptide component) were also prepared for comparison purposes.

2.5 Hybrid Gel Characterization

The formation of ionic liquid droplets and the morphological characteristics and differences between the hybrid gels containing the P1, P2 and P3 peptides were assessed via a ZEISS, Observer.Z1 Polarized Optical Microscope (POM) equipped with an Axiocam 503 color camera. Pictures were taken with crossed polarizers and in bright field and were processed with the ZEN 203 software.

Regarding the morphological stability of the hybrid gels upon storage over time, POM photos with crossed polarizers of the same region of interest were taken for a 30-day period. A custom-made python scrip (Python 3.6.2) was used to analyze the photos. The scrip uses binary images to calculate the differences between them.

2.6 VOC Sensing using Ionogels

All the prepared ionogels (peptide-based and controls) were assessed in an in-house tailor-made electrical e-nose device (Hussain et al., 2017). The device detects changes in the conductance upon VOC adsorption and desorption. The sensors were placed in a hermetically sealed array chamber and exposed to a sequence of six volatiles – hexane, benzene, toluene, xylene, ethanol and acetone – similar to the investigation of Ju et al. (Ju et al., 2015). The solvents were kept in a bath thermostated at 37°C and their respective vapors were pumped to the array chamber (exposure period) followed with ambient air via a second air pump (recovery period). The films were exposed to each gas analyte for 45 consecutive cycles, each cycle consisting of 5 sec of exposure followed by 10 sec of recovery, in total 7 min and 30 sec of test duration per VOC. The electrical signals of the sensors were acquired at a sampling rate of 90 Hz, and assays were performed in duplicates.

Processing and evaluation of the signals obtained was performed, using methods described in our previous publications (C. Esteves et al., 2019; S. I. C. J. Palma et al., 2019; Rodrigues et al., 2020; Santos et al., 2019b). Python programming tools were used to process the signals retrieved by the e-nose device.

For the evaluation of the sensors' performance regarding VOC identification, machine learning methods were applied to the individual cycles. Briefly, twelve features representative of the signals morphology were extracted from each cycle and used as input variables in an automatic classifier based on Support Vector Machines (SVM) algorithm, using a radial basis kernel and hyperparameters $C = 100$ and $\gamma = 0.1$. The dataset for each sensor formulation was composed by 30 cycles per VOC. Two thirds of this dataset were used as training set and one third as validation set for the automatic classifier. Accuracy bar plots, which exhibit the percentage of the correct predictions of the classifier were used to represent the sensors performance.

2.7 VOC Sensing using Hybrid Gels

The optical e-nose device is designed to monitor the light transmitted by the hybrid sensors and convert it into voltage. The detailed setup has been described in our previous works (Esteves et al., 2019; Hussain et al., 2017; Palma et al., 2019; Rodrigues et al., 2020). The sensors are placed in a hermetically sealed detection chamber and each one is paired with a polarizer and a corresponding analyzer. The VOC experiments, as well as the data analysis of the signals were conducted and processed as described in the previous section.

3 RESULTS AND DISCUSSION

3.1 Assessing VOC Selectivity in Ionogel: Electrical e-Nose

The affinity and selectivity of peptide P1 towards VOCs was firstly assessed by MP-SPR. Our results indicated a preferred binding of the peptide P1 towards VOCs following the order benzene < xylene < toluene < ethanol < acetone < hexane, as can be seen by the increase of the ΔmDeg values (see Table 1).

The three peptides were then incorporated into the ionogel gelatin matrices and spread as thin films onto interdigitated electrodes to be tested in an in-house developed electrical e-nose. VOCs adsorption to the ionogels affects the ion mobility within the materials. Therefore, the ionogels admittance changes and an electric response can be obtained. This is a reversible process upon VOC desorption and the basis for electrical VOC sensing with the electric E-nose (S. I. C. J. Palma et al., 2019).

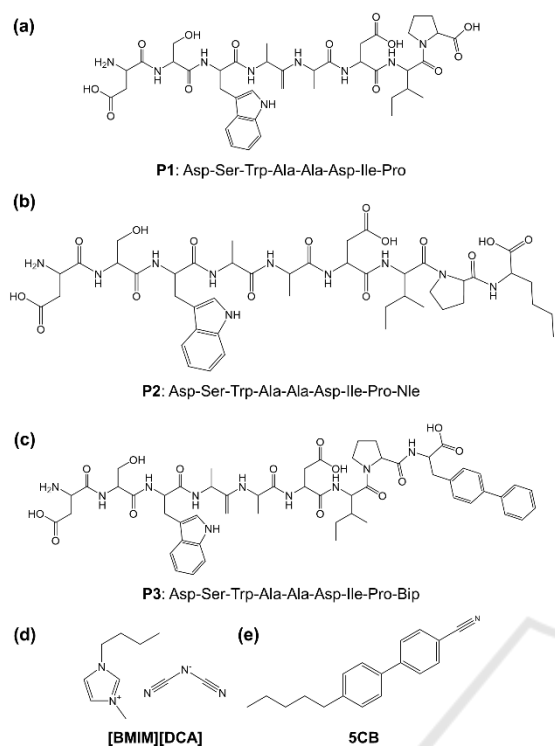


Figure 1: Chemical structure of (a) peptide 1, (b) peptide 2, (c) peptide 3, (d) ionic liquid 1-Butyl-3-methylimidazolium dicyanamide ([BMIM] [DCA]) and (e) liquid crystal 4-Cyano-4'-pentylbiphenyl (5CB).

Table 1: Summary-results of the interaction between the P1 functionalized Au surface and the VOCs. $\Delta m\text{Deg}$ (peptide-control) = $\Delta m\text{Deg}$ peptide - $\Delta m\text{Deg}$ control, where $\Delta m\text{Deg}$ peptide is the average of the signal measured at the 670 and 785 nm wavelengths in the peptide chamber, and $\Delta m\text{Deg}$ control is the average of the signal measured at the 670 and 785 nm wavelengths in the control chamber. Relative signal variation = the relative signal representing how much the signal increased on the peptide chamber, when compared to the control chamber.

VOCs	$\Delta m\text{Deg}$ (Peptide-Control)	Relative signal variation
Acetone	5.76 ± 2.16	0.21
Ethanol	2.20 ± 3.63	0.33
Benzene	32.54 ± 3.35	5.25
Xylene	14.69 ± 2.97	1.20
Toluene	5.61 ± 4.36	0.46
Hexane	6.19 ± 3.94	0.17

Through the sequential exposure of the peptide ionogel formulations to the 6 tested volatiles - hexane, benzene, toluene, xylene, ethanol and acetone - variations in the conductance of the sensors were monitored in real time and after signal processing (as

described in Materials and Methods section) typical relative amplitude responses are presented in Figure 2(a).

The sensor responses exhibit a variability in their profiles, characteristic of the corresponding gas analyte exposure. For example, all of the sensors during the linear 6C-alkyl chain hexane exposure respond with a downwards curve, while all other volatiles generate an upwards response signal. The majority of the sensors respond rather quickly (within seconds) upon VOCs exposure, during which most signals never reach a plateau, with the exception of xylene in control and P3 ionogels. Upon recovery, almost all sensor signals return to the baseline in a similar way.

After signal collection machine learning-based tools were implemented to analyze the data. The signals were divided into cycles and were then normalized. A set of features corresponding to the curve morphology (C. Esteves et al., 2019; S. I. C. J. Palma et al., 2019; Santos et al., 2019a) was extracted and used as input for an SVM-based automatic classifier. The accuracy % of correct VOC prediction is presented in an accuracy bar plot seen in Figure 2(b), depicting that the tested ionogel compositions exhibit distinct selectivity for the tested VOCs.

For example, P2 and P3-based sensors were able to discriminate and identify hexane and xylene, respectively, with an 100% accurate classification. This could be associated with the presence of the similar non-canonical aminoacid norleucine and biphenylalanine moieties in P2 and P3 peptides respectively and their similarity to the structure of the volatiles in question, possibly enhancing the interaction between the sensors and the volatiles. On a similar vein, the control ionogel provides great classification results for acetone and ethanol, with a 100% accuracy. The accuracy scores for the P1 ionogel were not as high (e.g. for toluene and xylene) which suggests that certain signal profiles produced by the formulation exhibited similar characteristics, thus not allowing the distinction of the corresponding analytes. Overall, the control ionogel formulation achieved the best global accuracy score (91%) followed by the P3-based ionogel (86%).

These results indicate that the incorporation of the peptides onto the gelatin ionogels did not yield an improvement of selectivity towards benzene and aromatic compounds. This is mainly due to the fact that the control ionogel already displayed excellent discriminating behavior towards the particular VOCs tested, as conductance and selectivity are already driven by the ionic liquid component.

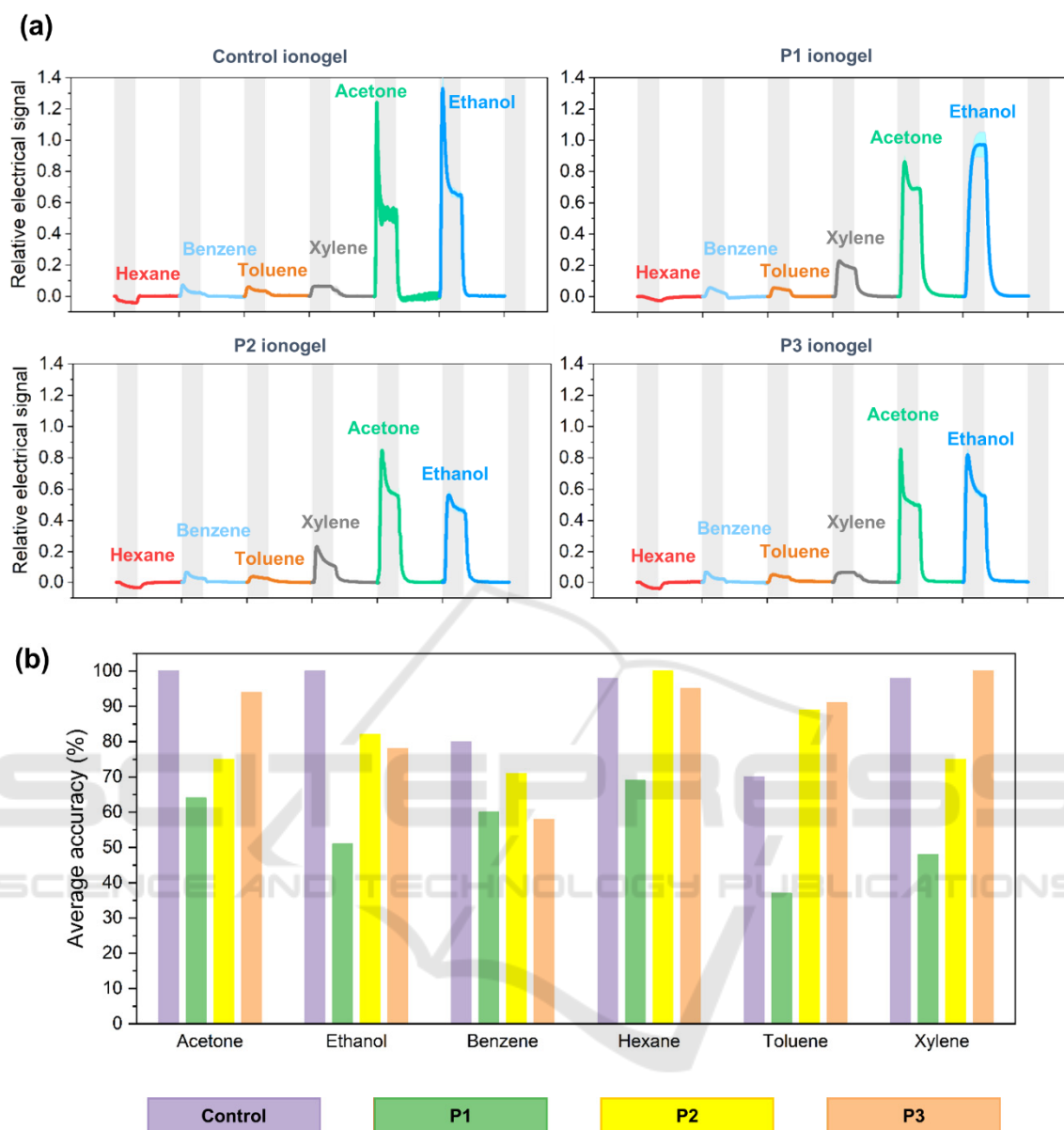


Figure 2: Electrical e-nose results for Control, P1, P2 and P3-based ionogels. (a) Typical cycle signals of all the sensors upon exposure to different VOCs. Each curve represents the average and standard deviation of at least 19 replicate cycles from the same sensor. VOC exposure periods (5 s) are highlighted in grey, and each cycle corresponds in total to 15 s. (b) Comparison of the VOC prediction accuracies obtained for all the ionogels tested in the electrical e-nose.

3.2 Assessing VOC Selectivity in Hybrid Gels: Optical e-Nose

The peptides P1, P2 and P3 were incorporated into hybrid gel formulations by simply adding them to the formulation and promoting autonomous self-assembly of the different moieties into the hybrid gel compartments. The formation of ionic liquid – liquid crystal droplets was observed by bright field and polarized optical microscopy (Figure 3).

All the hybrid gels (control and peptide-based) exhibit polydisperse 5CB droplets as previously noted (Esteves et al., 2019; Hussain et al., 2017; Palma et al., 2019), featuring a radial configuration which under the POM gives rise to a distinctive Maltese cross pattern (Drzaic, 1995). The characteristic core defect located in the center of the droplet can be observed in the bright field pictures (Esteves et al., 2019; Hussain et al., 2017) – seen in Figure 3 (a), (e) and (j). The radial droplet profile

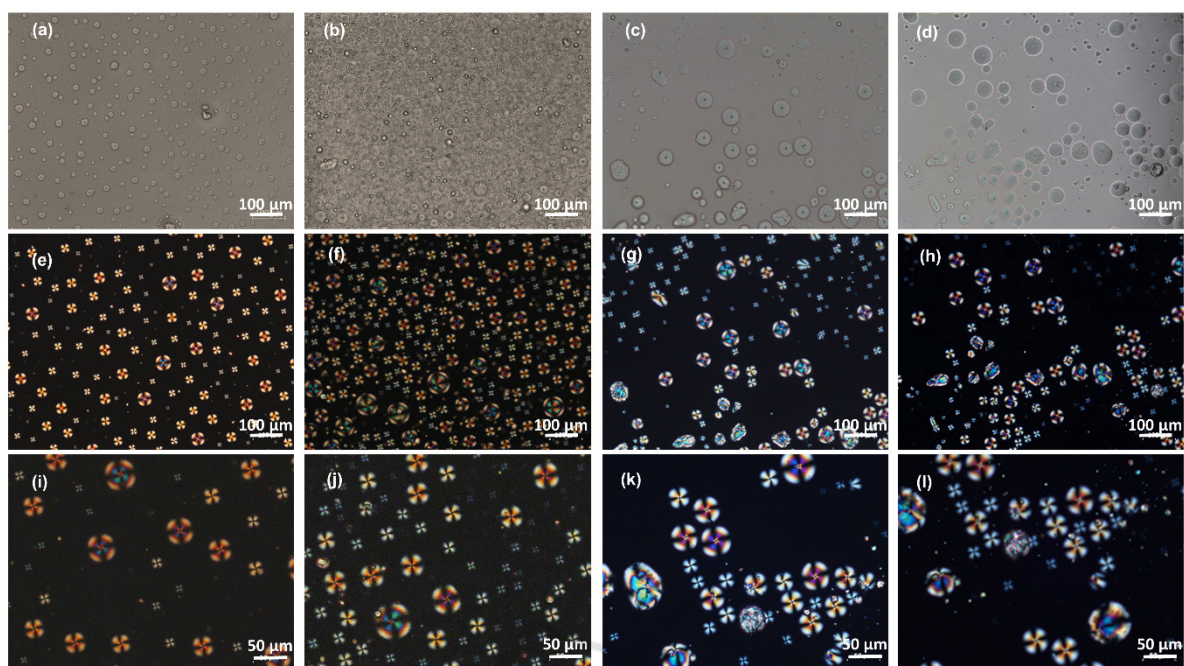


Figure 3: Representative POM images of control hybrid gel (a), (e) and (i), peptide 1 hybrid gel (b), (f) and (j), peptide 2 hybrid gel (c), (g) and (k) and peptide 3 hybrid gel (d), (h) and (l).

suggests that the liquid crystal molecules adopt a homeotropic alignment near the ionic liquid interface, which is attributed to the interactions occurring between the alkyl chain of the ionic liquid and 5CB (C. Esteves et al., 2019; Carina Esteves et al., 2020; A. Hussain et al., 2017).

We need to point out that in the case of P2-based and P3-based hybrid compositions, apart from the radial droplets, some irregularly shaped and randomly oriented droplets were also observed. This finding suggests that both the N1e (in the case of the P2 peptide) and Bip (in the case of the P3 peptide) moieties interfere with the liquid crystal anchoring on the ionic liquid interface.

The peptide-based hybrid gels were tested in the optical e-nose. Exposure to the tested gas analytes results in a disorganization of the liquid crystal component, triggering a phase transition to the isotropic state. The signal responses are the collaborative responses of the individual compartments of the gel formulations to the corresponding analyte. For example, hydrophobic VOCs, such as hexane and the aromatic benzene, xylene and toluene, are more likely to interact mainly with the oil phase formed by the liquid crystal molecules inside the droplets. Protic VOCs, and those forming hydrogen bonds (e.g. ethanol), tend to interact not only with the LC droplets but also with the gelatin matrix itself, as previously reported

(Esteves et al., 2019; Hussain et al., 2017). The sensor responses were repeatable and exhibited features (such as signal profile, response/recovery profile) characteristic of the tested volatiles.

Signal processing, analysis and presentation were conducted using the same tools as in the electrical e-nose results, described in the previous section. In Figure 4(a) relative amplitude responses for each tested hybrid peptide gel compositions and for all the studied gas analytes is shown. The baseline on each individual curve represents the initial light state of a sensor, due to the presence of the liquid crystal droplets. Upon VOC exposure the liquid crystal component becomes isotropic, thus it cannot alter the polarization of the transmitted light (which subsequently cannot pass through the analyzer). This generates an upwards response curve to a dark(er) state for the sensor.

It is possible to observe that each sensor holds a very characteristic amplitude signature signal, related to the different volatiles. For example, a delayed response upon analyte exposure is observed (e.g. hexane for control and P1-based hybrid gels), or the cases where a plateau in the response is reached (e.g. the control and P3-based sensors for all volatiles, with the exception of hexane and ethanol), and a very distinctive flat response from P1-based sensor towards ethanol.

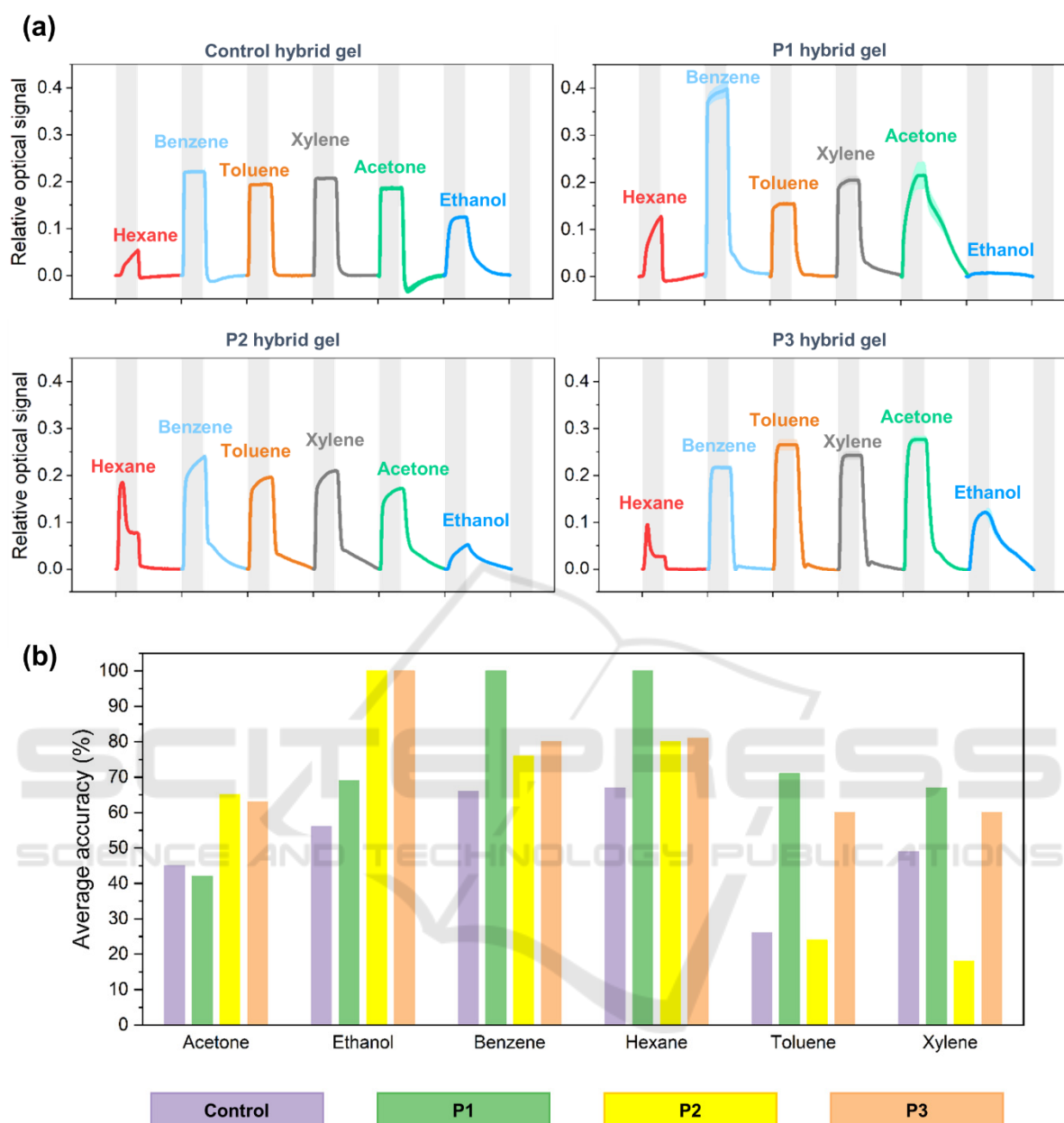


Figure 4: Optical e-nose results for the for Control, P1, P2 and P3-based hybrid gels. **(a)** Typical cycle signals of all the sensors upon exposure to different VOCs. Each curve represents the average and standard deviation of at least 19 replicate cycles from the same sensor. VOC exposure periods (5 s) are highlighted in grey, and each cycle corresponds in total to 15 s. **(b)** Comparison of the VOC prediction accuracies obtained for all the sensors tested in the optical e-nose.

Another interesting observation is that although the 10 s recovery period seems to be sufficient for the liquid crystal to completely recuperate from isotropisation in the control hybrid formulation (allowing the sensors signal to return to the initial baseline levels), the majority of the peptide-based sensors appear to take longer to completely recover within the 10 s period. This is evident in the case of

P1 sensors with benzene, xylene and acetone, and both P2 and P3 sensors with all volatiles – with the exception of hexane. It should be noted that this recovery pattern was not detected for the ionogel sensors previously analyzed.

When looking at the VOC prediction accuracy bar plot (seen in Figure 4(b)) it is noticeable that selectivity towards benzene and hexane from the P1-

based sensor was achieved. Overall, the P1-based hybrid gel was able to distinguish and classify all the tested volatiles presenting a 74% score of global accuracy.

4 CONCLUSIONS

In this work we studied the incorporation of peptides in two distinct groups of gas sensitive materials. Ionogels, comprised of gelatin and ionic liquid, tailored for electrical gas sensing and hybrid gels, containing gelatin, ionic liquid and liquid crystal, designed for optical gas sensing. A peptide (P1) known to discriminate single carbon deviations among benzene and derivatives was used as a model, along with two modified versions (P2 and P3). The set of ionogels were tested in an electrical e-nose, designed to monitor changes in the conductance of the sensors, and selectivity towards hexane and xylene was observed in the case of P2 and P3 ionogel sensors, respectively. Regarding the hybrid gels, the incorporation of peptide P1 did not disrupt the self-assembly of the ionic liquid crystal droplets (suggesting that peptide P1 is mainly distributed in the matrix), while the incorporation of peptides P2 and P3 disrupt some droplets, although the majority exhibit a radial configuration. The set of hybrid gels were tested in an optical e-nose, designed to monitor the light transmitted from the materials. An enhanced discrimination of benzene was observed for the P1-based gel and for ethanol in the case of both P2 and P3 hybrid gels. As a final note, we would like to highlight the complementarity of the two distinct gel formulations responses, since the combination of both optical and electrical prediction accuracies could provide the best classification accuracies for the tested VOCs. For example, the P2 ionogel was more

Table 2: Relative accuracy scores of VOC prediction from every ionogel and hybrid gel peptide sensors' tested. The relative accuracy score is defined as the difference between the peptide-based accuracy score and the control accuracy score.

VOCs	Relative accuracy ionogels (%)			Relative accuracy hybrid gels (%)		
	P1	P2	P3	P1	P2	P3
Acetone	-3	20	18	-36	-25	-6
Ethanol	13	44	44	-49	-18	-22
Benzene	34	10	14	-20	-9	-22
Xylene	33	13	14	-29	2	-3
Toluene	45	-2	34	-33	19	21
Hexane	18	-31	11	-50	-23	2

selective towards hexane and toluene whereas the P2 hybrid gel was more selective towards ethanol, suggesting that additional information and enhanced selectivity can be obtained regarding discrimination of volatiles, by using a combinatorial sensors array in a dual-mode e-nose. An overall view of the relative accuracy results from all sensors, regarding discrimination of each VOC, can be seen in Table 2.

ACKNOWLEDGEMENTS

This project has received funding from the European Research Council (ERC) under the EU Horizon 2020 research and innovation programme [grant reference SCENT-ERC-2014-STG-639123, (2015-2022)] and by national funds from FCT - Fundação para a Ciência e a Tecnologia, I.P., in the scope of the project UIDP/04378/2020 and UIDB/04378/2020 of the Research Unit on Applied Molecular Biosciences – UCIBIO and the project LA/P/0140/2020 of the Associate Laboratory Institute for Health and Bioeconomy - i4HB, which is financed by national funds from financed by FCT/MEC (UID/Multi/04378/2019). The authors thank FCT/MCTES for the PhD grants SFRH/BD/128687/2017 and PD/BD/139800/2018.

REFERENCES

- Barbosa, A. J. M., Oliveira, A. R., & Roque, A. C. A. (2018). Protein- and Peptide-Based Biosensors in Artificial Olfaction. *Trends in Biotechnology*, 36(12), 1244–1258. <https://doi.org/10.1016/j.tibtech.2018.07.004>
- Broza, Y. Y., Mochalski, P., Ruzsanyi, V., Amann, A., & Haick, H. (2015). Hybrid Volatolomics and Disease Detection. *Angewandte Chemie - International Edition*, 54(38), 11036–11048. <https://doi.org/10.1002/anie.201500153>
- Cruz, H., Califórnia, A., Pinto, A., Fonseca, J., Palmeira-De-Oliveira, J. G. A., Martinez-De-Oliveira, J., & Pereira, L. (2017). Development of e-nose biosensors based on organic semiconductors towards low-cost health care diagnosis in gynecological diseases. *Materials Today: Proceedings*, 4(11), 11544–11553. <https://doi.org/10.1016/j.matpr.2017.09.065>
- Cui, Y., Kim, S. N., Naik, R. R., & McAlpine, M. C. (2012). Biomimetic peptide nanosensors. *Accounts of Chemical Research*, 45(5), 696–704. <https://doi.org/10.1021/ar2002057>
- Dey, A. (2018). Semiconductor metal oxide gas sensors: A review. *Materials Science and Engineering B*, 229, 206–217. <https://doi.org/10.1016/j.mseb.2017.12.036>

- Drzaic, P. S. (1995). Nematic Configurations Within Droplets. In *Liquid Crystal Dispersions* (pp. 99–181). World Scientific.
- Esteves, C., Santos, G. M. C., Alves, C., Palma, S. I. C. J., Porteira, A. R., Filho, J., Costa, H. M. A., Alves, V. D., Morais, B. M., Ferreira, I., Gamboa, H., & Roque, A. C. A. (2019). Effect of film thickness in gelatin hybrid gels for artificial olfaction. *Materials Today Bio*, 1(December 2018), accepted manuscript. <https://doi.org/10.1016/j.mtbio.2019.100002>
- Esteves, Carina, Ramou, E., Porteira, A. R. P., Moura Barbosa, A. J., & Roque, A. C. A. (2020). Seeing the Unseen: The Role of Liquid Crystals in Gas-Sensing Technologies. *Advanced Optical Materials*, 8(11). <https://doi.org/10.1002/adom.201902117>
- Fitzgerald, J., & Fenniri, H. (2017). Cutting edge methods for non-invasive disease diagnosis using e-tongue and e-nose devices. *Biosensors*, 7(4). <https://doi.org/10.3390/bios7040059>
- Hussain, Abid, Semeano, A. T. S., Palma, S. I. C. J., Pina, A. S., Almeida, J., Medrado, B. F., Pádua, A. C. C. S., Carvalho, A. L., Dionísio, M., Li, R. W. C., Gamboa, H., Ulijn, R. V., Gruber, J., & Roque, A. C. A. (2017). Tunable Gas Sensing Gels by Cooperative Assembly. *Advanced Functional Materials*, 27(27), 1–9. <https://doi.org/10.1002/adfm.201700803>
- Ju, S., Lee, K. Y., Min, S. J., Yoo, Y. K., Hwang, K. S., Kim, S. K., & Yi, H. (2015). Single-carbon discrimination by selected peptides for individual detection of volatile organic compounds. *Scientific Reports*, 5, 9196. <https://doi.org/10.1038/srep09196>
- Krilaviciute, A., Heiss, J. A., Leja, M., Kupcinskas, J., Haick, H., & Brenner, H. (2015). Detection of cancer through exhaled breath: A systematic review. *Oncotarget*, 6(36), 38643–38657. <https://doi.org/10.18632/oncotarget.5938>
- Kuang, Z., Kim, S. N., Crookes-Goodson, W. J., Farmer, B. L., & Naik, R. R. (2010). Biomimetic chemosensor: Designing peptide recognition elements for surface functionalization of carbon nanotube field effect transistors. *ACS Nano*, 4(1), 452–458. <https://doi.org/10.1021/nn901365g>
- Palma, S. I. C. J., Esteves, C., Padua, A. C. C. S., Alves, C. M., Santos, G. M. C., Costa, H. M. A., Dionísio, M., Gamboa, H., Gruber, J., & Roque, A. C. A. (2019). Enhanced gas sensing with soft functional materials. *2019 IEEE International Symposium on Olfaction and Electronic Nose (ISOEN)*, 1–3. <https://doi.org/10.1109/ISOEN.2019.8823178>
- Palma, Susana I.C.J., Tragedo, A. P., Porteira, A. R., Frias, M. J., Gamboa, H., & Roque, A. C. A. (2018). Machine learning for the meta-analyses of microbial pathogens' volatile signatures. *Scientific Reports*, 8(1), 1–15. <https://doi.org/10.1038/s41598-018-21544-1>
- Park, S. J., Park, C. S., & Yoon, H. (2017). Chemo-electrical gas sensors based on conducting polymer hybrids. *Polymers*, 9(5), 155. <https://doi.org/10.3390/polym9050155>
- Rodrigues, R., Palma, S. I. C. J., G. Correia, V., Padrão, I., Pais, J., Banza, M., Alves, C., Deuermeier, J., Martins, C., Costa, H. M. A., Ramou, E., Silva Pereira, C., & Roque, A. C. A. (2020). Sustainable plant polyesters as substrates for optical gas sensors. *Materials Today Bio*, 8(August). <https://doi.org/10.1016/j.mtbio.2020.100083>
- Sankaran, S., Khot, L. R., & Panigrahi, S. (2012). Biology and applications of olfactory sensing system : A review. *Sensors and Actuators: B. Chemical*, 171–172, 1–17. <https://doi.org/10.1016/j.snb.2012.03.029>
- Santos, G., Alves, C., Pádua, A. C., Palma, S., Gamboa, H., & Roque, A. C. (2019a). An optimized e-nose for efficient volatile sensing and discrimination. *BIODEVICES 2019 - 12th International Conference on Biomedical Electronics and Devices, Proceedings; Part of 12th International Joint Conference on Biomedical Engineering Systems and Technologies, BIOSTEC 2019*, 36–46. <https://doi.org/10.5220/0007390700360046>
- Santos, G., Alves, C., Pádua, A. C., Palma, S., Gamboa, H., & Roque, A. C. (2019b). An optimized e-nose for efficient volatile sensing and discrimination. In A. Roque, A. Fred, & H. Gamboa (Eds.), *BIODEVICES 2019 - 12th International Conference on Biomedical Electronics and Devices, Proceedings; Part of 12th International Joint Conference on Biomedical Engineering Systems and Technologies, BIOSTEC 2019* (pp. 36–46). SCITEPRESS. <https://doi.org/10.5220/0007390700360046>
- Son, M., Lee, J. Y., Ko, H. J., & Park, T. H. (2017). Bioelectronic Nose: An Emerging Tool for Odor Standardization. *Trends in Biotechnology*, 35(4), 301–307. <https://doi.org/10.1016/j.tibtech.2016.12.007>
- van Hooren, M. R. A., Leunis, N., Brandsma, D. S., Dingemans, A. M. C., Kremer, B., & Kross, K. W. (2016). Differentiating head and neck carcinoma from lung carcinoma with an electronic nose: a proof of concept study. *European Archives of Oto-Rhino-Laryngology*, 273(11), 3897–3903. <https://doi.org/10.1007/s00405-016-4038-x>
- Vishinkin, R., & Haick, H. (2015). Nanoscale Sensor Technologies for Disease Detection via Volatolomics. *Small*, 11(46), 6142–6164. <https://doi.org/10.1002/smll.201501904>
- Capelli, L., Sironi, S., & Del Rosso, R. (2014). Electronic noses for environmental monitoring applications. *Sensors*, 14(11), 19979–20007. <https://doi.org/10.3390/s141119979>
- Chehri, A., Farjow, W., Mouftah, H. T., & Fernando, X. (2011). Design of wireless sensor network for mine safety monitoring. *2011 24th Canadian Conference on Electrical and Computer Engineering (CCECE), Niagara Falls, ONT*, 001532–001535. <https://doi.org/10.1109/CCECE.2011.6030722>
- Cui, Y., Kim, S. N., Naik, R. R., & McAlpine, M. C. (2012). Biomimetic peptide nanosensors. *Accounts of Chemical Research*, 45(5), 696–704. <https://doi.org/10.1021/ar2002057>
- Dey, A. (2018). Semiconductor metal oxide gas sensors: A review. *Materials Science and Engineering B*, 229, 206–217. <https://doi.org/10.1016/j.mseb.2017.12.036>

- Drzaic, P. S. (1995). Nematic Configurations Within Droplets. In *Liquid Crystal Dispersions* (pp. 99–181). World Scientific.
- Esteves, C., Santos, G. M. C., Alves, C., Palma, S. I. C. J., Porteira, A. R., Filho, J., Costa, H. M. A., Alves, V. D., Morais, B. M., Ferreira, I., Gamboa, H., & Roque, A. C. A. (2019). Effect of film thickness in gelatin hybrid gels for artificial olfaction. *Materials Today Bio*, 1(December 2018), accepted manuscript. <https://doi.org/10.1016/j.mtbio.2019.100002>
- Hussain, A., Semeano, A. T. S., Palma, S. I. C. J., Pina, A. S. P., Almeida, J., Medrado, B. F. F., Padua, A. C. C. S., Carvalho, A. L., Dionisio, M., Li, R. W. C., Gamboa, H., Ulijn, R. V., Gruber, J., & Roque, A. C. A. (2017). Tunable Gas Sensing Gels by Cooperative Assembly. *Advanced Functional Materials*, 27, 1700803. <https://doi.org/10.1002/adfm.201700803>
- Ju, S., Lee, K. Y., Min, S. J., Yoo, Y. K., Hwang, K. S., Kim, S. K., & Yi, H. (2015). Single-carbon discrimination by selected peptides for individual detection of volatile organic compounds. *Scientific Reports*, 5, 9196. <https://doi.org/10.1038/srep09196>
- Kuang, Z., Kim, S. N., Crookes-Goodson, W. J., Farmer, B. L., & Naik, R. R. (2010). Biomimetic chemosensor: Designing peptide recognition elements for surface functionalization of carbon nanotube field effect transistors. *ACS Nano*, 4(1), 452–458. <https://doi.org/10.1021/nn901365g>
- Lefferts, M. J., & Castell, M. R. (2015). Vapour sensing of explosive materials. *Analytical Methods*, 7(21), 9005–9017. <https://doi.org/10.1039/c5ay02262b>
- Palma, S. I. C. J., Esteves, C., Padua, A. C. C. S., Alves, C. M., Santos, G. M. C., Costa, H. M. A., Dionisio, M., Gamboa, H., Gruber, J., & Roque, A. C. A. (2019). Enhanced gas sensing with soft functional materials. *2019 IEEE International Symposium on Olfaction and Electronic Nose (ISOEN)*, 1–3. <https://doi.org/10.1109/ISOEN.2019.8823178>
- Park, S. J., Park, C. S., & Yoon, H. (2017). Chemo-electrical gas sensors based on conducting polymer hybrids. *Polymers*, 9(5), 155. <https://doi.org/10.3390/polym9050155>
- Rodrigues, R., Palma, S. I. C. J., G. Correia, V., Padrão, I., Pais, J., Banza, M., Alves, C., Deuermeier, J., Martins, C., Costa, H. M. A., Ramou, E., Silva Pereira, C., & Roque, A. C. A. (2020). Sustainable plant polyesters as substrates for optical gas sensors. *Materials Today Bio*, 8(August). <https://doi.org/10.1016/j.mtbio.2020.100083>
- Sankaran, S., Khot, L. R., & Panigrahi, S. (2012). Biology and applications of olfactory sensing system: A review. *Sensors and Actuators: B. Chemical*, 171–172, 1–17. <https://doi.org/10.1016/j.snb.2012.03.029>
- Santos, G., Alves, C., Pádua, A. C., Palma, S., Gamboa, H., & Roque, A. C. (2019a). An optimized e-nose for efficient volatile sensing and discrimination. *BIODEVICES 2019 - 12th International Conference on Biomedical Electronics and Devices, Proceedings; Part of 12th International Joint Conference on Biomedical Engineering Systems and Technologies, BIOSTEC 2019*, 36–46. <https://doi.org/10.5220/0007390700360046>
- Santos, G., Alves, C., Pádua, A. C., Palma, S., Gamboa, H., & Roque, A. C. (2019b). An optimized e-nose for efficient volatile sensing and discrimination. In A. Roque, A. Fred, & H. Gamboa (Eds.), *BIODEVICES 2019 - 12th International Conference on Biomedical Electronics and Devices, Proceedings; Part of 12th International Joint Conference on Biomedical Engineering Systems and Technologies, BIOSTEC 2019* (pp. 36–46). SCITEPRESS. <https://doi.org/10.5220/0007390700360046>
- Son, M., Lee, J. Y., Ko, H. J., & Park, T. H. (2017). Bioelectronic Nose: An Emerging Tool for Odor Standardization. *Trends in Biotechnology*, 35(4), 301–307. <https://doi.org/10.1016/j.tibtech.2016.12.007>
- van Hooren, M. R. A., Leunis, N., Brandsma, D. S., Dingemans, A. M. C., Kremer, B., & Kross, K. W. (2016). Differentiating head and neck carcinoma from lung carcinoma with an electronic nose: a proof of concept study. *European Archives of Oto-Rhino-Laryngology*, 273(11), 3897–3903. <https://doi.org/10.1007/s00405-016-4038-x>
- Zampolli, S., Elmi, I., Ahmed, F., Passini, M., Cardinali, G. C., Nicoletti, S., & Dori, L. (2004). An electronic nose based on solid state sensor arrays for low-cost indoor air quality monitoring applications. *Sensors and Actuators, B: Chemical*, 101(1–2), 39–46. <https://doi.org/10.1016/j.snb.2004.02.024>